

# New Ruthenium Carbonyl Clusters Containing Unusual $\mu_5$ -Sulfido-, $\mu_4$ -Benzynes-, and Thianthrene-Derived Ligands: Insertion of Ruthenium into the Thianthrene Ring by C–S Activation

Mohammad R. Hassan,<sup>†</sup> Shariff E. Kabir,<sup>\*,†</sup> Brian K. Nicholson,<sup>\*,‡</sup> Ebbe Nordlander,<sup>§</sup> and Md. Nazim Uddin<sup>†</sup>

Department of Chemistry, Jahangirnagar University, Savar, Dhaka 1342, Bangladesh,  
Department of Chemistry, University of Waikato, Hamilton, New Zealand, and Inorganic Chemistry  
Research Group, Center for Chemistry and Chemical Engineering, Lund University, Box 124, SE 221 00,  
Lund, Sweden

Received May 12, 2007

Treatment of  $[\text{Ru}_3(\text{CO})_{12}]$  with thianthrene in refluxing toluene afforded  $[(\mu_4\text{-S})\text{Ru}_4(\mu\text{-CO})_2(\text{CO})_9(\mu_4\text{-}\eta^2\text{-C}_6\text{H}_4)]$  (**1**),  $[(\mu_5\text{-S})\text{Ru}_6(\mu\text{-CO})_2(\text{CO})_{15}(\mu\text{-}\eta^3\text{-C}_{12}\text{H}_8\text{S})]$  (**2**), and  $[(\mu_5\text{-S})\text{Ru}_5(\mu\text{-CO})_2(\text{CO})_{11}(\mu\text{-}\eta^3\text{-C}_{12}\text{H}_8\text{S})(\mu_4\text{-}\eta^2\text{-C}_6\text{H}_4)]$  (**3**) in 18%, 8%, and 16% yields, respectively. Thermolysis of **2** in refluxing heptane gave compounds **1** and **3**. A similar thermolysis of **3** in refluxing toluene gave **1** in 90% yield. Treatment of **3** with neat MeCN afforded the labile compound  $[(\mu_5\text{-S})\text{Ru}_5(\mu\text{-CO})_2(\text{CO})_{10}(\mu\text{-}\eta^3\text{-C}_{12}\text{H}_8\text{S})(\mu_4\text{-}\eta^2\text{-C}_6\text{H}_4)(\text{MeCN})]$  (**4**) in 73% yield. The reaction of **4** with  $\text{P}(\text{OMe})_3$  gave the substitution product  $[(\mu_5\text{-S})\text{Ru}_5(\mu\text{-CO})_2(\text{CO})_{10}(\mu\text{-}\eta^3\text{-C}_{12}\text{H}_8\text{S})(\mu_4\text{-}\eta^2\text{-C}_6\text{H}_4)\{\text{P}(\text{OMe})_3\}]$  (**5**) in 52% yield. Compounds **1**–**4** have been structurally characterized. Compound **1** contains a  $\mu_4$ -capping sulfido and a  $\mu_4\text{-}\eta^2$ -benzynes ligand, whereas **3**, **4**, and **5** contain  $\mu_5$ -sulfido and  $\mu_4\text{-}\eta^2$ -benzynes ligands. The latter three compounds provide rare examples of  $\mu_5$ -sulfido and metal-assisted opening of the thianthrene ligand on polynuclear centers. In compounds **1**, **3**, and **4** the  $\mu_4\text{-}\eta^2$ -benzynes ligand is perpendicular to the  $\text{Ru}_4$  face of the clusters and represents a previously uncharacterized bonding mode for benzynes.

## Introduction

The continuing considerable interest in transition metal complexes containing sulfur donor ligands is stimulated by their significant relevance to biological and industrial processes.<sup>1</sup> Sulfur-coordinated transition metal complexes are the active centers in many redox reactions in life processes. Such centers have been modeled with complexes containing cyclic polydentate sulfur ligands.<sup>2</sup> In addition, hydrodesulfurization (HDS) is also important for both industrial and environmental reasons; it is performed on a massive scale for the removal of sulfur from organosulfur compounds in petroleum-based feedstocks.<sup>3,4</sup> Given that aromatic S-heterocycles are among the most difficult impurities to remove,<sup>5</sup> a large number of model studies con-

cerning transition metal thiophene, benzothiophene, and substituted benzothiophene complexes have appeared in the literature.<sup>4–16</sup> Stone and co-workers<sup>13,14</sup> were the first to demonstrate the reactivity of organometallic clusters with thiophenic molecules, such as thiophene and benzothiophene, to produce ring-opened or desulfurized thiophene-containing transition metal complexes.  $[\text{Ru}_3(\text{CO})_{12}]$  has been reported to react with thiophene and benzothiophene to afford both ring-opened and desulfurized thiophene-containing complexes.<sup>17–21</sup> Transition

<sup>†</sup> Jahangirnagar University.

<sup>‡</sup> University of Waikato.

<sup>§</sup> Lund University.

(1) (a) Rauchfuss, T. B. *Inorg. Chem.* **2004**, *43*, 14. (b) *Transition Metal Sulfur Chemistry-Biological and Industrial Significance*; Stiefel, E. I., Matsumoto, K., Eds.; ACS Symposium Series 653; American Chemical Society: Washington, DC, 1996. (c) Howard, J. B.; Rees, D. C. *Chem. Rev.* **1996**, *96*, 2965. (d) Sellman, D.; Sutter, J. *Acc. Chem. Res.* **1997**, *30*, 460. (e) Bianchini, C.; Meli, A. *Acc. Chem. Res.* **1998**, *31*, 109.

(2) Abel, E. W.; Beer, P. D.; Moss, I.; Orrell, K. G.; Sik, V.; Bates, P. A.; Hursthouse, M. B. *J. Organomet. Chem.* **1998**, *341*, 559, and references therein.

(3) (a) Reynolds, M. A.; Guzei, I. A.; Angelici, R. J. *Inorg. Chem.* **2003**, *42*, 2191. (b) Reynolds, M. A.; Guzei, I. A.; Angelici, R. J. *J. Chem. Soc., Chem. Commun.* **2000**, 513. (c) Reynolds, M. A.; Guzei, I. A.; Angelici, R. J. *Organometallics* **2001**, *20*, 1071. (d) Chen, J.; Angelici, R. J. *Organometallics* **1999**, *18*, 5721. (e) Prins, R.; De Beer, V. H. J.; Somorjai, G. A. *Catal. Rev.-Sci. Eng.* **1989**, *31*, 1. (f) Topsøe, H.; Clausen, B. S.; Massoth, F. E. In *Hydrotreating Catalysis*; Springer-Verlag: Berlin, 1996. (g) Dullaghan, C. A.; Sun, S.; Welden, B.; Schweigart, D. A. *Angew. Chem., Int. Ed. Engl.* **1996**, *35*, 212.

(4) Angelici, R. J. In *Encyclopedia of Inorganic Chemistry*, 2nd ed.; King, R. B., Ed.; Wiley: New York, 2005; Vol. 3, p 1860.

(5) Mills, R. C. A.; Boncella, J. M. *Chem. Commun.* **2001**, 1506.

(6) Angelici, R. J. *Organometallics* **2001**, *20*, 1259.

(7) Angelici, R. J. *Coord. Chem. Rev.* **1990**, *105*, 61.

(8) Rauchfuss, T. B. *Prog. Inorg. Chem.* **2004**, *43*, 14.

(9) Janak, K. E.; Tanski, J. M.; Churchill, D. G.; Perkin, G. J. *J. Am. Chem. Soc.* **2002**, *124*, 4182.

(10) (a) Spera, M. L.; Harman, W. D. *J. Am. Chem. Soc.* **1997**, *119*, 8843. (b) Spera, M. L.; Harman, W. D. *Organometallics* **1999**, *18*, 2988.

(11) Bianchini, C.; Herrera, V.; Jimenez, M.; Meli, A.; Sanchez-Delgado, R. A.; Vizza, F. *J. Am. Chem. Soc.* **1995**, *117*, 8567.

(12) Kabir, S. E.; Miah, M. A.; Sarkar, N. C.; Hussain, G. M. G.; Hardcastle, K. I.; Nordlander, E.; Rosenberg, E. *Organometallics* **2005**, *24*, 3315.

(13) Kaesz, H. D.; King, R. B.; Manuel, T. A.; Nichols, L. D.; Stone, F. G. A. *J. Am. Chem. Soc.* **1960**, *82*, 4749.

(14) King, R. B.; Stone, F. G. A. *J. Am. Chem. Soc.* **1960**, *82*, 4557.

(15) Ogilvy, A. E.; Draganjac, M.; Rauchfuss, T. B.; Wilson, F. R. *Organometallics* **1988**, *7*, 1171.

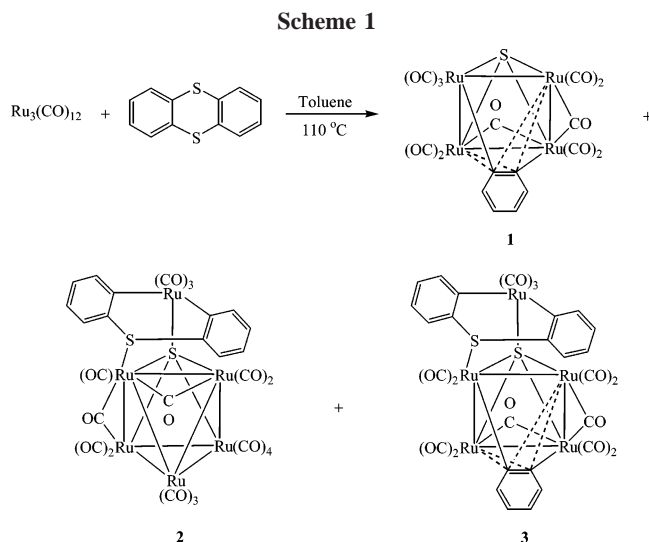
(16) Brorson, M.; King, J. D.; Kiriakidou, K.; Prestopino, F.; Nordlander, E. In *Metal Clusters in Chemistry*; Braunstein, P., Oro, L. A., Raithby, P. R., Eds.; Wiley-VCH: Weinheim, 1999; Vol. 2, pp 741–781.

(17) (a) Fish, R. H.; Baralt, E.; Smith, S. J. *Organometallics* **1991**, *10*, 54. (b) Baralt, E.; Smith, S. J.; Hurwitz, J.; Horvath, I. T.; Fish, R. H. *J. Am. Chem. Soc.* **1992**, *114*, 5187.

(18) (a) Arce, A. J.; De Sanctis, Y.; Karam, A.; Deeming, A. J. *Angew. Chem., Int. Ed. Engl.* **1994**, *33*, 1381. (b) Arce, A. J.; Arrojo, P.; De Sanctis, Y.; Karam, A.; Deeming, A. J. *J. Chem. Soc., Dalton Trans.* **1992**, 2423.

(19) Arce, A. J.; Karam, A.; De Sanctis, Y.; Capparelli, M. V.; Deeming, A. J. *Inorg. Chim. Acta* **1999**, *285*, 277.

(20) Adams, R. D.; Pompeo, M. P.; Wu, W.; Yamamoto, J. H. *J. Am. Chem. Soc.* **1993**, *115*, 8207.



metal insertions into C–S bonds to give thioether complexes have been studied in the context of desulfurization of cyclic thioethers, which are found as impurities in crude oil. The reactions of  $[\text{Ru}_3(\text{CO})_{12}]$  with cyclic thioethers, such as 1,3,5-trithiacyclohexane, 1,4,7-trithiacyclononane, 1,5,9-trithiacyclododecane, and 1,5,9,13-tetrithiacyclohexadecane, resulted in a remarkable variety of structures depending on the ligand.<sup>22–24</sup> 1,3,5-Trithiacyclohexane replaces three axial carbonyls to form  $[\text{Ru}_3(\text{CO})_9(\mu_3-\eta^3\text{-1,3,5-trithiacyclohexane})]$ , whereas the coordination of 1,3-dithiacyclohexane involves activation of a C–H bond between the sulfur atoms to give  $[(\mu\text{-H})\text{Ru}_3(\text{CO})_9(\mu_3-\eta^3\text{-1,3-dithiacyclohexane})]$ . 1,4,7-Trithiacyclononane loses a  $\text{H}_2\text{CCH}_2$  fragment during the complexation, and two sulfur bridges are formed between two ruthenium atoms.<sup>23</sup> To our knowledge, however, no examples have been reported in the literature concerning the reactivity between thianthrene and transition metal carbonyl complexes. We were prompted to scrutinize the reactivity of thianthrene from several points of view. Although in previous studies, all the reactions were carried out with thiophene derivatives containing one sulfur atom in the ring, we chose thianthrene, which contains two sulfur atoms in the ring, proffering further possibilities to undergo C–S bond cleavage.

## Results and Discussion

The reaction of  $[\text{Ru}_3(\text{CO})_{12}]$  with thianthrene in refluxing toluene for 30 min resulted in the isolation of three new clusters,  $[(\mu_4\text{-S})\text{Ru}_4(\mu\text{-CO})_2(\text{CO})_9(\mu_4-\eta^2\text{-C}_6\text{H}_4)]$  (**1**),  $[(\mu_5\text{-S})\text{Ru}_6(\mu\text{-CO})_2(\text{CO})_{15}(\mu\text{-}\eta^3\text{-C}_{12}\text{H}_8\text{S})]$  (**2**), and  $[(\mu_5\text{-S})\text{Ru}_5(\mu\text{-CO})_2(\text{CO})_{11}(\mu\text{-}\eta^3\text{-C}_{12}\text{H}_8\text{S})(\mu_4-\eta^2\text{-C}_6\text{H}_4)]$  (**3**), in 18%, 8%, and 16% yields, respectively (Scheme 1).

Compounds **1–3** have been characterized by a combination of spectroscopic data and single-crystal X-ray diffraction studies. The molecular structure of **1** is shown in Figure 1, crystal data are given in Table 1, and selected bond distances and bond angles are listed in Table 2.

The cluster core consists of a slightly folded rhomboid of Ru atoms (fold angle  $24^\circ$ ), capped on the concave face by a  $\mu_4\text{-S}$  atom. Because of the fold, the Ru–S distances show two

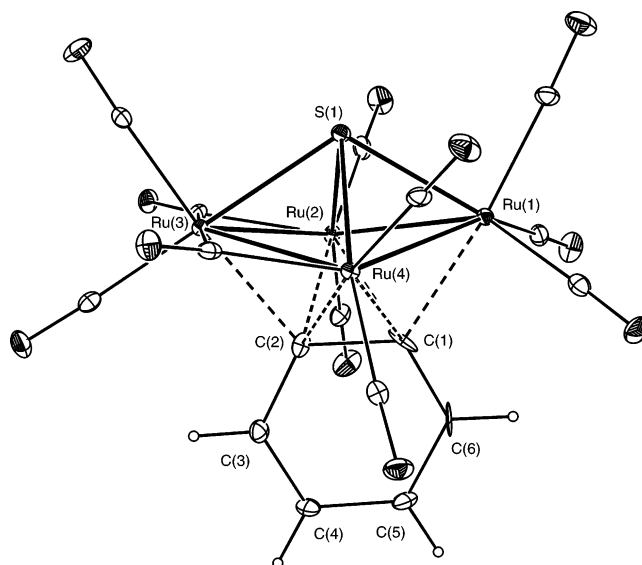


**Figure 1.** Structure of  $[(\mu_4\text{-S})\text{Ru}_4(\text{CO})_{11}(\mu_4-\eta^2\text{-C}_6\text{H}_4)]$  (**1**).

short bonds (av  $2.410 \text{ \AA}$ ) from Ru(1) and Ru(3) and two longer bonds (av  $2.493 \text{ \AA}$ ) from Ru(2) and Ru(4). The 11 CO ligands are arranged so that one of the Ru atoms has three terminal COs, while the other three Ru atoms have two terminal COs with the remaining two in bridging positions along two adjacent sides of the pseudosquare. This ligand arrangement is the same as in  $[(\mu_4\text{-S})_2\text{Ru}_4(\text{CO})_9(\text{PMe}_2\text{Ph})_2]$ ,<sup>25</sup> although a more symmetrical distribution of 11 CO ligands over four Ru atoms can be found in  $[(\mu_4\text{-S})(\mu_4\text{-PhP})\text{Ru}_4(\text{CO})_{11}]$ .<sup>26</sup> As expected, the CO-bridged Ru–Ru bonds are shorter (av  $2.739 \text{ \AA}$ ) than the unbridged ones (av  $2.804 \text{ \AA}$ ).

The convex side of the  $\text{Ru}_4$  unit is attached to a benzyne ligand, bonded as a  $4e$  donor in a  $\mu_4-\eta^2$ -mode, which appears to be unprecedented. The plane of the benzyne group is essentially perpendicular to the least-squares plane through the four ruthenium atoms (dihedral angle  $87.3^\circ$ ), and the ligand lies diagonally across the  $\text{Ru}_4$  pseudosquare. Partial disorder in the structure of **1** lowers the accuracy of the bond parameters involving the benzyne group, so a more detailed analysis of the bonding will be deferred until the discussion of structures **3** and **4** below, since they also have the same geometry for the  $\text{Ru}_4$  benzyne fragment.

The spectroscopic data of **1** are consistent with the solid-state structure. The  $^1\text{H}$  NMR spectrum contains two multiplets at  $\delta$  7.44 and 6.40 in a 1:1 ratio, due to the rotation of the benzyne group like the ones reported for  $[\text{Ru}_4(\mu\text{-CO})(\text{CO})_9(\mu_4-\eta^2\text{-PCH}_2\text{CH}_2\text{PPh}_2)(\mu_4-\eta^4\text{-C}_6\text{H}_4)]$ .<sup>27</sup> The variable-temperature NMR studies on **1** indicate that the fluxionality of the  $\mu_4-\eta^2$ -benzyne ligand could not be frozen out even at  $-80^\circ\text{C}$  because of the fact that the asymmetry in this structure arises only from the presence of the bridging carbonyls, so CO scrambling can average the nominally unsymmetrical environment of the benzyne ligand. In contrast, the inherent asymmetry in  $[\text{Ru}_4(\mu\text{-CO})(\text{CO})_9(\mu_4-\eta^2\text{-PCH}_2\text{CH}_2\text{PPh}_2)(\mu_4-\eta^4\text{-C}_6\text{H}_4)]$  is due to the coordination of the  $\mu_4-\eta^2\text{-PCH}_2\text{CH}_2\text{PPh}_2$  ligand, which inhibits averaging in this square tetraruthenium carbonyl compound at low temperature.<sup>27</sup> The fluxionality in cluster **1** is well-supported

(21) Adams, R. D.; Qu, X. *Organometallics* **1995**, *14*, 2238.

(22) Rossi, S.; Kallinen, K.; Pursiainen, J.; Pakkanen, T. T.; Pakkanen, T. A. *J. Organomet. Chem.* **1992**, *440*, 367.

(23) Adams, R. D.; Falloon, S. B.; McBride, K. T.; Yamamoto, J. H. *Organometallics* **1995**, *14*, 1739.

(24) Adams, R. D.; Yamamoto, J. H. *Organometallics* **1995**, *14*, 3704.

(25) Adams, R. D.; Babin, J. E.; Tasi, M. *Inorg. Chem.* **1986**, *25*, 4514.

(26) Van Gastel, F.; Agocs, L.; Cherkas, A. A.; Corrigan, J. F.; Doherty, S.; Ramachandran, R.; Taylor, N. J.; Carty, A. J. *J. Cluster Sci.* **1991**, *2*, 131.

(27) Sanchez-Cabrera, G.; Zuno-Cruz, F. J.; Rosales-Hoz, M. J.; Bakhmutov, V. I. *J. Organomet. Chem.* **2002**, *660*, 153.

Table 1. Crystal Data and Refinement Details for Clusters 1–4

|   | Ru <sub>4</sub> cluster 1  | Ru <sub>6</sub> cluster 2   | Ru <sub>5</sub> cluster 3  | Ru <sub>5</sub> cluster 4   |
|---|--|---|--|---|
| formula   | C <sub>17</sub> H <sub>4</sub> O <sub>11</sub> Ru <sub>4</sub> S | C <sub>29</sub> H <sub>8</sub> O <sub>17</sub> Ru <sub>6</sub> S <sub>2</sub> | C <sub>31</sub> H <sub>12</sub> O <sub>13</sub> Ru <sub>5</sub> S <sub>2</sub> | C <sub>32</sub> H <sub>15</sub> NO <sub>12</sub> Ru <sub>5</sub> S <sub>2</sub> ·0.5CH <sub>2</sub> Cl <sub>2</sub> |
| <i>M<sub>r</sub></i>  | 820.54   | 1298.89   | 1161.88  | 1217.38   |
| <i>T</i> (K)  | 93(2)  | 87(2)   | 89(2)  | 89(2)   |
| cryst syst  | monoclinic   | monoclinic  | triclinic  | monoclinic  |
| space group   | <i>C2/c</i>  | <i>P2<sub>1</sub>/n</i>   | <i>P</i> $\bar{1}$   | <i>P2<sub>1</sub>/c</i>   |
| <i>a</i> (Å)  | 14.4705(4)   | 11.456(1)   | 9.4548(1)  | 18.2731(2)  |
| <i>b</i> (Å)  | 10.5311(3)   | 15.880(1)   | 10.5298(1)   | 11.7362(2)  |
| <i>c</i> (Å)  | 28.5654(9)   | 19.179(1)   | 19.1888(2)   | 17.7859(3)  |
| $\alpha$ (deg)  | 90   | 90  | 90.504(1)  | 90  |
| $\beta$ (deg)   | 91.963(1)  | 90.261(1)   | 101.411(1)   | 108.452(1)  |
| $\gamma$ (deg)  | 90   | 90  | 115.811(1)   | 90  |
| <i>V</i> (Å <sup>3</sup> )                                  | 4350.5(2)  | 3489.1(4)   | 1676.01(2)   | 3618.2(1)   |
| <i>Z</i>  | 8  | 4   | 2  | 4   |
| $\rho$ (g cm <sup>-3</sup> )                                | 2.506  | 2.473   | 2.302  | 2.235   |
| $\mu$ (mm <sup>-1</sup> )                                   | 2.877  | 2.73  | 2.39   | 2.29  |
| size (mm <sup>3</sup> )                                     | 0.36 × 0.16 × 0.06   | 0.34 × 0.26 × 0.12  | 0.28 × 0.18 × 0.16   | 0.32 × 0.24 × 0.08  |
| <i>F</i> (000)  | 3088   | 2456  | 1108   | 2332  |
| $\theta_{\max}$ (deg)                                       | 27.5   | 26.4  | 26.5   | 26.4  |
| no. of reflns collected                                     | 31 675   | 33 278  | 16 388   | 21 239  |
| <i>T</i> <sub>max</sub> , <i>T</i> <sub>min</sub>           | 0.846, 0.424   | 0.588, 0.441  | 0.701, 0.554   | 0.838, 0.528  |
| no. of unique reflns  | 5003 ( <i>R</i> <sub>int</sub> 0.026)                            | 7121 ( <i>R</i> <sub>int</sub> 0.026)   | 6842 ( <i>R</i> <sub>int</sub> 0.026)  | 7388 ( <i>R</i> <sub>int</sub> 0.035)   |
| no. of params   | 298  | 487   | 460  | 497   |
| <i>R</i> <sub>1</sub> [ <i>I</i> > 2 $\sigma$ ( <i>I</i> )] | 0.0392   | 0.0219  | 0.0216   | 0.0309  |
| <i>wR</i> <sub>2</sub> (all data)                           | 0.0948   | 0.0511  | 0.0552   | 0.0694  |
| GOF on <i>F</i> <sup>2</sup>                                | 1.225  | 1.058   | 1.054  | 1.074   |

by the <sup>13</sup>C NMR spectrum, exhibiting two signals at  $\delta$  150.0 and 127.8, even at  $-80$  °C, for the benzyne ligand. In addition this spectrum shows a single CO resonance at  $\delta$  201.4, even at  $-80$  °C, which demonstrates very facile scrambling among the CO groups. This peak is in the same region as the chemical shift reported for the CO ligands in [Ru<sub>4</sub>( $\mu$ -CO)(CO)<sub>9</sub>( $\mu_4$ - $\eta^2$ -PCH<sub>2</sub>CH<sub>2</sub>PPh<sub>2</sub>)( $\mu_4$ - $\eta^4$ -C<sub>6</sub>H<sub>4</sub>)].<sup>27</sup> The FAB mass spectrum of **1** shows a molecular ion peak at *m/z* 822 consistent with its formulation, while an ESI mass spectrum with added NaOMe as an ionization aid<sup>28</sup> gave a strong [M + OMe]<sup>-</sup> ion at *m/z* 853.

The structure of compound **2** is depicted in Figure 2, crystal data are given in Table 1, and selected bond distances and bond angles are listed in Table 2. Compound **2** has an octahedral SRu<sub>5</sub> core like that found in [( $\mu_4$ -S)Ru<sub>5</sub>(CO)<sub>15</sub>] and [( $\mu_4$ -S)Ru<sub>5</sub>(CO)<sub>14</sub>]<sup>2-</sup> as well as in the more complex structures [( $\mu_4$ -S)-Ru<sub>6</sub>(CO)<sub>18</sub>] and [( $\mu_4$ -S)Ru<sub>7</sub>(CO)<sub>21</sub>].<sup>29,30</sup> However, for **2** there is the further coordination of the S to another Ru atom to give an overall  $\mu_5$ -environment. The extra ruthenium is attached to a doubly metalated diphenyl sulfide ligand that has arisen from loss of one sulfur atom from thianthrene. This ligand is further coordinated through the remaining sulfur atom to one of the ruthenium atoms in the lower core. There are few  $\mu_5$ -S examples involving metal carbonyl clusters known; perhaps the closest analogues would be the complexes reported by Adams et al., where a [( $\mu_4$ -S)Os<sub>5</sub>(CO)<sub>15</sub>] or a [( $\mu_4$ -S)<sub>2</sub>Ru<sub>4</sub>(CO)<sub>9</sub>(PMe<sub>2</sub>Ph)<sub>2</sub>] cluster is linked through a sulfur atom to a W(CO)<sub>4</sub>PR<sub>3</sub> fragment.<sup>31</sup>

The spectroscopic data of **2** are fully consistent with the solid-state structure. The <sup>1</sup>H NMR spectrum contains four equal intensity multiplets at  $\delta$  7.87, 7.50, 7.22, and 7.00 each integrating for two hydrogens. The FAB and ESI mass spectra contain the appropriate [M]<sup>+</sup> and [M + OMe]<sup>-</sup> peaks, respectively, for the molecular mass of 1300 Da. Thermolysis of **2** in refluxing heptane affords **1** and **3**. It is interesting to note that compound

**1** results from the displacement of the unique Ru(CO)<sub>3</sub> fragment by a benzyne moiety, which in turn arises from C–S and Ru–C bond cleavage of the fragmented top half, Ru(CO)<sub>3</sub>(C<sub>12</sub>H<sub>8</sub>S), of **2**. Compound **3** formally results from the displacement of the unique Ru(CO)<sub>3</sub> fragment of **2** by a benzyne moiety.

The structure of compound **3** is depicted in Figure 3, crystal data are given in Table 1, and selected bond distances and bond angles are listed in Table 2. Compound **3** represents a unique example of a pentaruthenium cluster containing a capping  $\mu_5$ -S ligand, a  $\mu_4$ -benzyne ligand, and a Ru(CO)<sub>3</sub> fragment incorporating a doubly cyclometalated ligand arising from the loss of a sulfur atom from thianthrene. The structure of **3** therefore combines the features of the  $\mu_4$ - $\eta^2$ -C<sub>6</sub>H<sub>4</sub> part of **1** with the  $\mu^5$ -SRu(CO)<sub>3</sub>[(C<sub>6</sub>H<sub>4</sub>)<sub>2</sub>S]<sub>2</sub> part of **2** about the Ru<sub>4</sub> rhomboid. The distribution of CO ligands around the Ru<sub>4</sub> unit in **3** is the same as in **1**, and the fold angle is only slightly less at 22°, so the variation in Ru–S and Ru–Ru bonds follows a very similar pattern. The details of the bonding to the C<sub>6</sub>H<sub>4</sub> ligand are discussed below.

Thermolysis of **3** in refluxing toluene affords **1**, indicating that the formation of **1** proceeds via the intermediate formation of **2** and **3**.

The spectroscopic data of **3** are consistent with the solid-state structure. In agreement with the presence of a benzyne and a Ru(C<sub>12</sub>H<sub>8</sub>S) ligand in **3**, the <sup>1</sup>H NMR spectrum contains six equal intensity multiplets at  $\delta$  7.87, 7.49, 7.38, 7.12, 6.81, and 6.26. The formulation of **3** is supported by its FAB and ESI mass spectrum, which confirm a mass of 1163 Da.

The reaction of **3** with neat acetonitrile and subsequent chromatographic separation afforded the acetonitrile derivative [( $\mu_5$ -S)Ru<sub>5</sub>( $\mu$ -CO)<sub>2</sub>(CO)<sub>10</sub>( $\mu$ - $\eta^3$ -C<sub>12</sub>H<sub>8</sub>S)( $\mu_4$ - $\eta^2$ -C<sub>6</sub>H<sub>4</sub>)(MeCN)] (**4**) (Scheme 2) in 73% yield, which has been characterized by spectroscopic data and a single-crystal X-ray diffraction study. The molecular structure of **4** is depicted in Figure 3, crystal data are given in Table 1, and selected bond distances and bond angles are compared with the corresponding ones of **3** in Table 2. The salient features of **4** in the solid state remain essentially the same as those of **3** except that a CO ligand from the apical Ru(CO)<sub>3</sub> group of **3** has been substituted by an acetonitrile ligand.

(28) Henderson, W.; McIndoe, J. S.; Nicholson, B. K.; Dyson, P. J. *J. Chem. Soc., Dalton Trans.* **1998**, 519.

(29) Adams, R. D.; Babin, J. E.; Tasi, M. *Organometallics* **1988**, *7*, 503.

(30) Bodensieck, U.; Meister, G.; Stoeckli-Evans, H.; Süss-Fink, G. *J. Chem. Soc., Dalton Trans.* **1992**, 2131.

(31) Adams, R. D.; Babin, J. E.; Natarajan, K.; Tasi, M.; Wang, J.-G. *Inorg. Chem.* **1987**, *26*, 3708.

**Table 2. Bond Lengths [Å] and Angles [deg] for Clusters 1–4**

| Ru <sub>4</sub> Cluster 1        |            |          |                   |            |           |
|----------------------------------|------------|----------|-------------------|------------|-----------|
| Bond Lengths                     |            |          |                   |            |           |
| Ru(1)–C(1)                       | 2.157(6)   |          | Ru(1)–S(1)        | 2.4007(16) |           |
| Ru(1)–Ru(4)                      | 2.7723(7)  |          | Ru(1)–Ru(2)       | 2.8395(7)  |           |
| Ru(2)–C(2)                       | 2.345(6)   |          | Ru(2)–C(1)        | 2.405(7)   |           |
| Ru(2)–S(1)                       | 2.4915(16) |          | Ru(2)–Ru(3)       | 2.7442(7)  |           |
| Ru(3)–C(2)                       | 2.248(6)   |          | Ru(3)–S(1)        | 2.4197(16) |           |
| Ru(3)–Ru(4)                      | 2.7339(7)  |          | Ru(4)–C(2)        | 2.333(6)   |           |
| Ru(4)–C(1)                       | 2.440(6)   |          | Ru(4)–S(1)        | 2.4937(15) |           |
| C(1)–C(6)                        | 1.376(11)  |          | C(1)–C(2)         | 1.482(9)   |           |
| C(2)–C(3)                        | 1.409(9)   |          | C(3)–C(4)         | 1.369(9)   |           |
| C(4)–C(5)                        | 1.424(10)  |          | C(5)–C(6)         | 1.382(10)  |           |
| Bond Angles                      |            |          |                   |            |           |
| Ru(1)–S(1)–Ru(3)                 | 116.27(6)  |          | Ru(2)–S(1)–Ru(4)  | 93.75(5)   |           |
| Ru(1)–S(1)–Ru(2)                 | 70.93(4)   |          | Ru(3)–S(1)–Ru(2)  | 67.92(4)   |           |
| Ru(1)–S(1)–Ru(4)                 | 68.97(4)   |          | Ru(3)–S(1)–Ru(4)  | 67.60(4)   |           |
| C(6)–C(1)–C(2)                   | 118.5(6)   |          | C(3)–C(2)–C(1)    | 117.1(6)   |           |
| C(4)–C(3)–C(2)                   | 122.9(6)   |          | C(3)–C(4)–C(5)    | 119.2(6)   |           |
| C(6)–C(5)–C(4)                   | 119.9(6)   |          | C(1)–C(6)–C(5)    | 122.5(6)   |           |
| Ru <sub>6</sub> Cluster 2        |            |          |                   |            |           |
| Bond Lengths                     |            |          |                   |            |           |
| Ru(1)–C(1)                       | 2.131(3)   |          | Ru(1)–C(7)        | 2.133(3)   |           |
| Ru(1)–S(1)                       | 2.4372(7)  |          | Ru(2)–S(1)        | 2.3923(7)  |           |
| Ru(2)–S(2)                       | 2.4432(7)  |          | Ru(2)–Ru(5)       | 2.7820(3)  |           |
| Ru(2)–Ru(6)                      | 2.7900(3)  |          | Ru(2)–Ru(3)       | 2.8048(3)  |           |
| Ru(3)–S(1)                       | 2.4112(7)  |          | Ru(3)–Ru(6)       | 2.7845(3)  |           |
| Ru(3)–Ru(4)                      | 2.7951(3)  |          | Ru(4)–S(1)        | 2.4162(7)  |           |
| Ru(4)–Ru(5)                      | 2.7624(3)  |          | Ru(4)–Ru(6)       | 2.8462(3)  |           |
| Ru(5)–S(1)                       | 2.4337(7)  |          | Ru(5)–Ru(6)       | 2.8716(3)  |           |
| S(2)–C(2)                        | 1.790(3)   |          | S(2)–C(8)         | 1.791(3)   |           |
| Bond Angles                      |            |          |                   |            |           |
| C(1)–Ru(1)–C(7)                  | 88.58(10)  |          | C(2)–S(2)–C(8)    | 104.23(13) |           |
| C(2)–S(2)–Ru(2)                  | 109.37(9)  |          | C(8)–S(2)–Ru(2)   | 108.51(9)  |           |
| Ru <sub>5</sub> Clusters 3 and 4 |            |          |                   |            |           |
| 3                                |            | 4        |                   |            |           |
| Bond Lengths                     |            |          |                   |            |           |
| Ru(1)–C(81)                      | 2.118(3)   | 2.119(4) | Ru(1)–S(1)        | 2.364(1)   | 2.375(1)  |
| Ru(1)–S(2)                       | 2.407(1)   | 2.402(1) | Ru(1)–Ru(2)       | 2.847(1)   | 2.848(1)  |
| Ru(1)–Ru(4)                      | 2.855(1)   | 2.827(1) | Ru(2)–C(82)       | 2.338(3)   | 2.370(4)  |
| Ru(2)–S(1)                       | 2.474(1)   | 2.481(1) | Ru(2)–C(81)       | 2.493(3)   | 2.375(4)  |
| Ru(2)–Ru(3)                      | 2.737(3)   | 2.757(1) | Ru(3)–C(82)       | 2.256(3)   | 2.260(4)  |
| Ru(3)–S(1)                       | 2.437(1)   | 2.448(1) | Ru(3)–Ru(4)       | 2.750(1)   | 2.737(4)  |
| Ru(4)–C(82)                      | 2.335(3)   | 2.322(4) | Ru(4)–C(81)       | 2.415(3)   | 2.516(4)  |
| Ru(4)–S(1)                       | 2.464(1)   | 2.474(1) | Ru(5)–C(61)       | 2.124(3)   | 2.125(4)  |
| Ru(5)–C(71)                      | 2.132(3)   | 2.085(4) | Ru(5)–S(1)        | 2.435(1)   | 2.456(1)  |
| S(2)–C(66)                       | 1.783(3)   | 1.787(4) | S(2)–C(76)        | 1.785(3)   | 1.781(4)  |
| C(81)–C(86)                      | 1.439(4)   | 1.444(5) | C(81)–C(82)       | 1.447(4)   | 1.438(5)  |
| C(82)–C(83)                      | 1.449(4)   | 1.449(5) | C(83)–C(84)       | 1.360(4)   | 1.357(6)  |
| C(84)–C(85)                      | 1.410(4)   | 1.405(6) | C(85)–C(86)       | 1.359(4)   | 1.354(6)  |
| Bond Angles                      |            |          |                   |            |           |
| C(61)–Ru(5)–C(71)                | 88.3(1)    | 89.3(2)  | Ru(1)–S(1)–Ru(3)  | 118.22(3)  | 117.09(4) |
| Ru(1)–S(1)–Ru(4)                 | 72.48(2)   | 71.30(3) | Ru(3)–S(1)–Ru(4)  | 68.27(2)   | 67.55(3)  |
| Ru(1)–S(1)–Ru(2)                 | 72.05(2)   | 71.79(3) | Ru(3)–S(1)–Ru(2)  |            | 67.73(2)  |
| Ru(4)–S(1)–Ru(2)                 | 96.97(2)   | 96.39(3) | C(66)–S(2)–C(76)  |            | 103.7(2)  |
| C(86)–C(81)–C(82)                | 118.0(2)   | 118.3(3) | C(81)–C(82)–C(83) |            | 116.6(2)  |
| C(84)–C(83)–C(82)                | 122.9(3)   | 122.1(4) | C(83)–C(84)–C(85) | 120.0(3)   | 120.5(4)  |
| C(86)–C(85)–C(84)                | 120.2(3)   | 120.4(4) | C(85)–C(86)–C(81) |            | 122.4(3)  |

The main effects are a lengthening of the S(1)–Ru(5) bond by 0.021 Å (presumably because of increased steric interactions with the cluster core) and a shortening of the Ru(5)–C(71) bond by 0.047 Å (because of the lower *trans* influence of an N- versus a C-bonded *trans* ligand). The fold angle in the Ru<sub>4</sub> rhomboid is 21.5°, and the benzyne ligand plane forms a dihedral angle of 86.7° with the Ru<sub>4</sub> least-squares plane. This part of the structure is discussed below.

The spectroscopic data of **4** are consistent with its solid-state molecular structure. Most informative is its <sup>1</sup>H NMR spectrum, which displays four doublets at δ 7.78 (*J* = 7.6 Hz), 7.71 (*J* = 7.6 Hz), 7.36 (*J* = 7.4 Hz), and 7.18 (*J* = 7.4 Hz) and four

triplets at δ 7.05 (*J* = 7.4 Hz), 6.94 (*J* = 7.6 Hz), 6.78 (*J* = 7.4 Hz), and 6.69 (*J* = 7.6 Hz), each integrating for one proton, assignable to the protons of the thianthrene ring, and two multiplets at δ 7.52 and 6.23, each integrating for two protons, assignable to the protons of the benzyne ring. A singlet at δ 2.39 was also observed in the <sup>1</sup>H NMR for the coordinated CH<sub>3</sub>-CN protons. The ESI mass spectrum of **4**, after derivatization with NaOMe, shows ions associated with the loss of CH<sub>3</sub>CN and addition of MeOH or CO (see Experimental Section). These suggest the MeCN ligand is very labile since rearrangements of this type are unusual under the mild electrospray conditions.



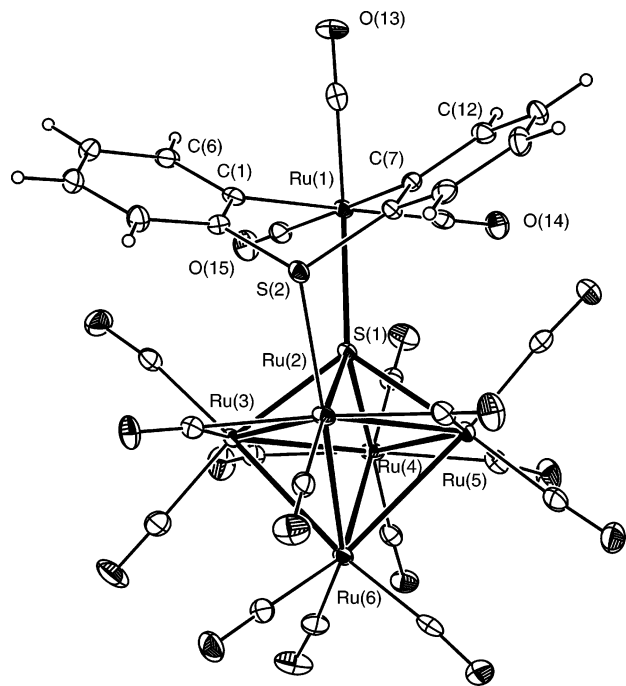


**Figure 2.** Structure of  $[(\mu_5\text{-S})\text{Ru}_6(\text{CO})_{16}(\mu\text{-}\eta^3\text{-C}_{12}\text{H}_8\text{S})]$  (**2**).

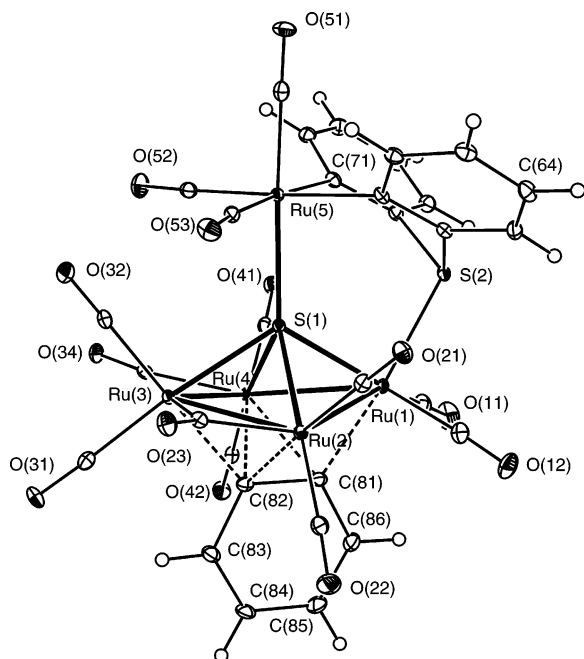
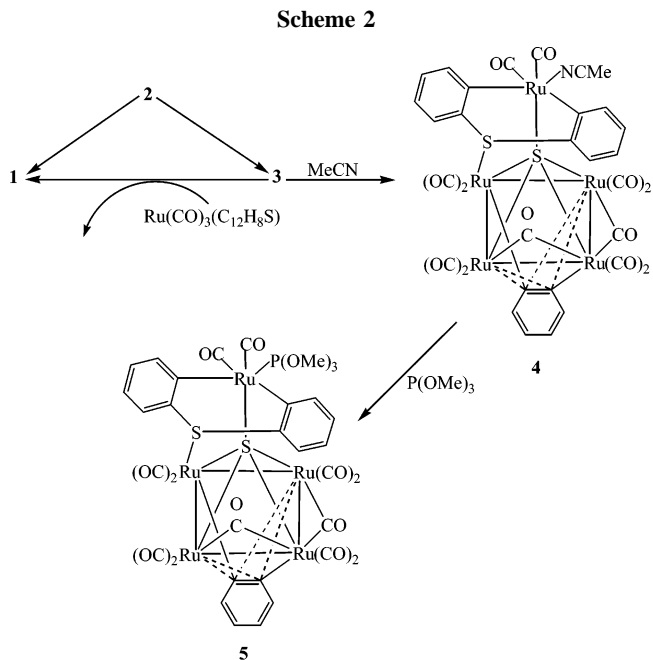


**Figure 3.** Structure of  $[(\mu_5\text{-S})\text{Ru}_5(\text{CO})_{13}(\mu\text{-}\eta^3\text{-C}_{12}\text{H}_8\text{S})(\mu_4\text{-}\eta^2\text{-C}_6\text{H}_4)]$  (**3**).

To confirm the lability of the acetonitrile ligand in **4**, we carried out the reaction of this complex with trimethylphosphite. As expected, the reaction of **4** with excess  $\text{P}(\text{OMe})_3$  afforded the substitution product  $[(\mu_5\text{-S})\text{Ru}_5(\mu\text{-CO})_2(\text{CO})_{10}(\mu\text{-}\eta^3\text{-C}_{12}\text{H}_8\text{S})(\mu_4\text{-}\eta^2\text{-C}_6\text{H}_4)\{\text{P}(\text{OMe})_3\}]$  (**5**) in 52% yield. This has been characterized by elemental analysis,  $^1\text{H}$  NMR,  $^{31}\text{P}\{^1\text{H}\}$  NMR, infrared, and mass spectroscopic data. The resonances corresponding to the benzyne and  $\text{C}_{12}\text{H}_8\text{S}$  protons are observed, in the  $^1\text{H}$  NMR spectrum, as six sets of equal intensity multiplets at  $\delta$  7.84, 7.50, 7.40, 7.03, 6.74, and 6.23 and a doublet resonance due to the methyl protons of the trimethyl phosphite ligand at  $\delta$  3.77 ( $J = 10.3$  Hz). The  $^{31}\text{P}\{^1\text{H}\}$  NMR displays a



singlet at  $\delta$  127.7 for the  $\text{P}(\text{OMe})_3$  ligand. The formulation of the cluster is also supported by its ESI mass spectrum, which shows  $[\text{M} + \text{Na}]^+$  and  $[\text{M} + \text{OMe}]^-$  peaks for  $\text{M} = 1259$  Da.

The most novel feature of the structures of clusters **1**, **3**, and **4** is the  $\mu_4\text{-}\eta^2\text{-C}_6\text{H}_4$  ligand, which appears to have a previously uncharacterized bonding mode. The availability of the three related structures, all with the same bonding, confirms that this is the preferred arrangement for this type of cluster and is not simply a crystal-packing artifact. In the following discussion the parameters from **3** and **4** will be used since those of **1** are less precise, although they follow the same pattern. Figure 5 illustrates the arrangement of the ligand above the  $\text{Ru}_4$  face of the cluster. Notable features include the following: (i) the plane of the  $\text{C}_6\text{H}_4$  ligand is essentially perpendicular to the least-squares plane through  $\text{Ru}(1\text{--}4)$  (av dihedral angle  $88^\circ$ ); (ii) the ligand is arranged almost diagonally across the pseudosquare

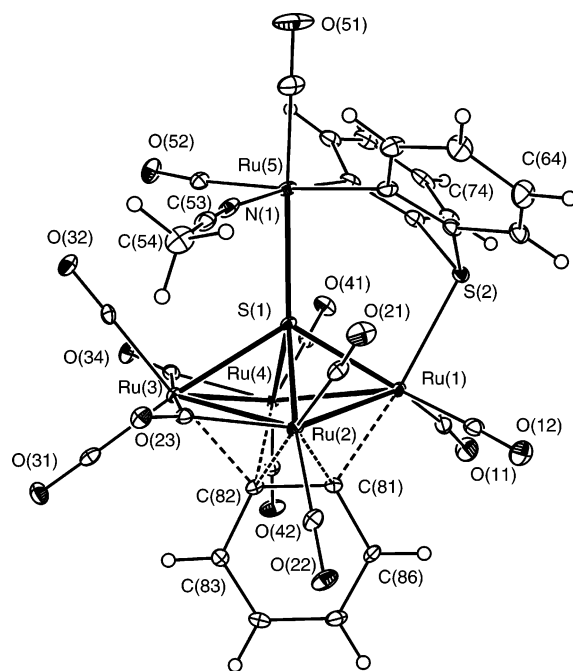


**Figure 4.** Structure of  $[(\mu_5\text{-S})\text{Ru}_5(\text{CO})_{12}(\mu\text{-}\eta^3\text{-C}_{12}\text{H}_8\text{S})(\mu_4\text{-}\eta^2\text{-C}_6\text{H}_4)(\text{MeCN})]$  (**4**).

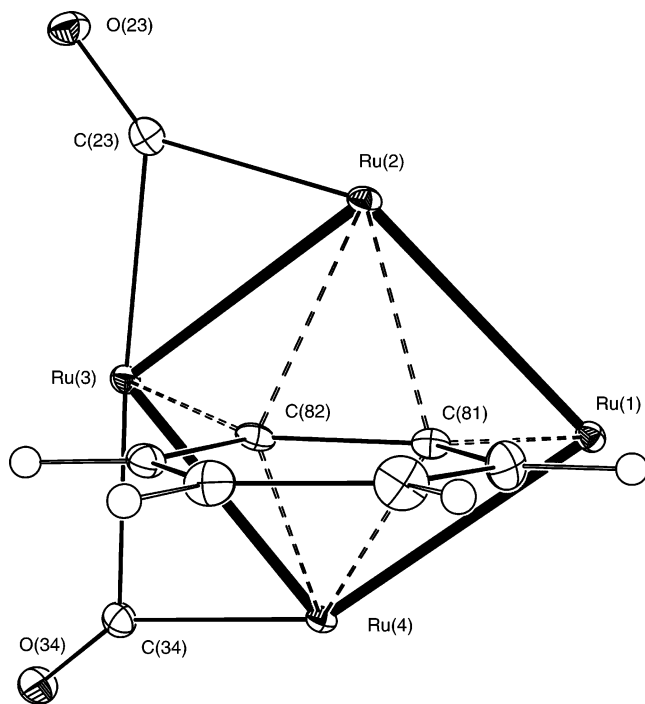


**Figure 5.** Orientation of the  $\mu_4\text{-}\eta^2$ -benzynes ligand on the  $\text{Ru}_4$  face of clusters **1**, **3**, and **4**.

face; (iii) there are two short Ru–C bonds, Ru(1)–C(81) and Ru(3)–Ru(82) (2.12 and 2.26 Å, respectively), and four longer ones (av 2.39 Å); (iv) the ligand is slightly closer to Ru(1) than Ru(3), presumably because of the unsymmetrical arrangement of the CO ligands, which gives Ru(3) a higher formal coordination number; (v) the remaining carbon atoms of the ring are too far away from the ruthenium atoms for any interaction; and (vi) there is significant bond alternation in the  $\text{C}_6$  ring, with C(83)–C(84) and C(85)–C(86) at 1.36 Å significantly shorter than C(82)–C(83), C(84)–C(85), and C(81)–C(86), which average 1.43 Å. All of this points to the benzynes ligand acting as a four-electron ligand, forming Ru–C  $\sigma$ -bonds to Ru(1) and Ru(3) and sharing the formal C(81)–C(82)  $\pi$ -bond with Ru(2) and Ru(4).

There are several previous examples of benzynes ligands attached to  $\text{M}_4$  faces of clusters, but as far as we are aware, they all have a tilted aryl group, aligned so the edge is parallel to one of the M–M sides and with further  $\pi$ -bonding to the other two Ru atoms, to give  $\mu_4\text{-}\eta^4\text{-6e}$  bonding of the benzynes.<sup>27,32</sup> The bonding in the present examples is more closely paralleled by complexes where a simple alkyne is bonded diagonally across a  $\text{Ru}_4$  square face, with  $[(\mu_4\text{-S})(\mu_4\text{-}\eta^2\text{-PhCCH})\text{Ru}_4(\text{CO})_{11}]$  providing a particularly close analogue.<sup>33</sup> Cullen et al.<sup>34</sup> have reported the cluster  $[(\mu_4\text{-As}\{\text{naphthyl}\})(\mu_4\text{-}\eta^2\text{-naphthyl})\text{Ru}_4(\text{CO})_{11}]$ , in which the naphthyl ligand is behaving as a  $\mu_4\text{-}\eta^2\text{-4e}$  ligand which is mildly tilted to give an angle of 75.3° to the  $\text{Ru}_4$  plane, compared with the more usual ca. 50° in the  $\mu_4\text{-}\eta^4\text{-6e}$  mode discussed above for earlier benzynes species and the ca. 90° in clusters **1** and **3–5**. This example

(32) For some representative examples see: Knox, S. A. R.; Lloyd, B. R.; Morton, D. A. V.; Nicholls, S. M.; Orpen, A. G.; Vinas, J. M.; Weber, M.; Williams, G. K. J. *Organometal. Chem.* **1990**, *394*, 385. Bruce, M. I.; Humphrey, P. A.; Shawkataly, O. b.; Snow, M. R.; Tiekink, E. R. T.; Cullen, W. R. *Organometallics* **1990**, *9*, 2910. Diz, E. L.; Neels, A.; Stoeckli-Evans, H.; Süß-Fink, G. *Inorg. Chem. Commun.* **2002**, *5*, 414.

(33) Adams, R. D.; Babin, J. E.; Tasi, M.; Wolfe, T. A. *Organometallics* **1987**, *6*, 2228.

(34) Cullen, W. R.; Rettig, S. J.; Zheng, T. C. *Organometallics* **1995**, *14*, 1466.

also differs in that the naphthyl ligand lies parallel to one of the sides of the  $\text{Ru}_4$  square face, rather than diagonally, and has a different disposition of the carbonyl ligands, with only one  $\mu\text{-CO}$  ligand rather than the two in the present examples. Only  $[(\mu_4\text{-PPh})(\mu_4\text{-}\eta^2\text{-C}_5\text{SH}_2)\text{Ru}_4(\text{CO})_{11}]$ , containing a thiophyne ligand, provides a direct analogue of a  $\mu_4\text{-}\eta^2\text{-4e}$  aryl arrangement lying perpendicularly and diagonally across the square face.<sup>35</sup>

It is not at all clear why this arrangement should be preferred in **1**, **3**, and **4**, since there was no indication of CO elimination, followed by a tilting of the benzynes ligand to give the more common  $\eta^4$ -arrangement, even under the relatively forcing conditions of synthesis.

## Experimental Section

**General Comments.** Unless otherwise stated, all the reactions were performed under a nitrogen atmosphere using standard Schlenk techniques. Solvents were dried and distilled prior to use by standard methods. Thianthrene was purchased from Aldrich and  $[\text{Ru}_3(\text{CO})_{12}]$  from Strem. Infrared spectra were recorded on a Shimadzu FTIR 8101 spectrophotometer.  $^1\text{H}$  and  $^{31}\text{P}\{^1\text{H}\}$  NMR spectra were recorded on Varian Unity Plus 500 and Bruker DPX 400 instruments. All chemical shifts are reported in  $\delta$  units with reference to the residual protons of the deuterated solvents for proton and to external 85%  $\text{H}_3\text{PO}_4$  for  $^{31}\text{P}$  chemical shifts. Elemental analyses were performed by the Microanalytical Laboratories, University College London. Mass spectra were recorded on a Fisons Platform II ESI mass spectrometer, with MeOH as mobile phase and NaOMe added as an ionization aid.<sup>28</sup> The  $m/z$  values reported are the strongest in the isotope envelope, and formulations were confirmed by matching isotope patterns with simulated ones generated with ISOTOPE.<sup>36</sup> Fast atom bombardment mass spectra were obtained on a JEOL SX-102 spectrometer using 3-nitrobenzyl alcohol as matrix and CsI as calibrant.

**Reaction of  $[\text{Ru}_3(\text{CO})_{12}]$  with Thianthrene.** To a toluene solution (30 mL) of  $[\text{Ru}_3(\text{CO})_{12}]$  (200 mg, 0.313 mmol) was added thianthrene (68 mg, 0.314 mmol), and the reaction mixture was heated to reflux at 110 °C for 30 min. The solvent was removed under reduced pressure and the residue chromatographed by TLC on silica gel. Elution with hexane/ $\text{CH}_2\text{Cl}_2$  (9:1 v/v) developed three bands. The first band afforded  $[(\mu_4\text{-S})\text{Ru}_4(\mu\text{-CO})_2(\text{CO})_9(\mu_4\text{-}\eta^2\text{-C}_6\text{H}_4)]$  (**1**) (48 mg, 18%) as red crystals after recrystallization from hexane/ $\text{CH}_2\text{Cl}_2$  at  $-4$  °C. Anal. Calcd for  $\text{C}_{17}\text{H}_4\text{O}_{11}\text{Ru}_4\text{S}$ : C, 24.88; H, 0.49. Found: C, 24.98; H, 0.62. IR ( $\nu\text{CO}$ ,  $\text{CH}_2\text{Cl}_2$ ): 2091 s, 2056 vs, 2040 vs, 1997 s  $\text{cm}^{-1}$ .  $^1\text{H}$  NMR ( $\text{CDCl}_3$ ):  $\delta$  7.44 (m, 2H), 6.40 (m, 2H). FAB-MS:  $m/z$  822  $[\text{M}]^+$ . ESI-MS:  $m/z$  853  $[\text{M} + \text{OMe}]^-$ . The second band gave  $[(\mu_5\text{-S})\text{Ru}_6(\mu\text{-CO})_2(\text{CO})_{15}(\mu\text{-}\eta^3\text{-C}_{12}\text{H}_8\text{S})]$  (**2**) (32 mg, 8%) as black crystals after recrystallization from hexane/ $\text{CH}_2\text{Cl}_2$  at  $-4$  °C. Anal. Calcd for  $\text{C}_{29}\text{H}_8\text{O}_{17}\text{Ru}_6\text{S}_2$ : C, 26.82; H, 0.62. Found: C, 26.95; H, 0.77. IR ( $\nu\text{CO}$ ,  $\text{CH}_2\text{Cl}_2$ ): 2098 s, 2074 s, 2047 vs, 2015 s, 2002 s, 1885 w, 1849 w  $\text{cm}^{-1}$ .  $^1\text{H}$  NMR ( $\text{CDCl}_3$ ):  $\delta$  7.87 (m, 2H), 7.50 (m, 2H), 7.22 (m, 2H), and 7.00 (m, 2H). FAB-MS:  $m/z$  1300  $[\text{M}]^+$ ; ESI-MS:  $m/z$  1331  $[\text{M} + \text{OMe}]^-$ . The third band gave  $[(\mu_5\text{-S})\text{Ru}_5(\mu\text{-CO})_2(\text{CO})_{11}(\mu\text{-}\eta^3\text{-C}_{12}\text{H}_8\text{S})(\mu_4\text{-}\eta^2\text{-C}_6\text{H}_4)]$  (**3**) (58 mg, 16%) as parallelepiped crystals after recrystallization from hexane/ $\text{CHCl}_3$  at  $-4$  °C. Anal. Calcd for  $\text{C}_{31}\text{H}_{12}\text{O}_{13}\text{Ru}_5\text{S}_2$ : C, 32.05; H, 1.04. Found: C, 32.29; H, 1.16. IR ( $\nu\text{CO}$ ,  $\text{CH}_2\text{Cl}_2$ ): 2096 s, 2066 w, 2042 vs, 2017 s, 1998 s, 1972 w, 1848 m  $\text{cm}^{-1}$ .  $^1\text{H}$  NMR ( $\text{CDCl}_3$ ):  $\delta$  7.87 (m, 2H), 7.49 (m, 2H), 7.38 (m, 2H), 7.12 (m, 2H), 6.81 (m, 2H), 6.26 (m, 2H). MS (FAB):  $m/z$  1163  $[\text{M}]^+$ ; ESI-MS: 1194  $[\text{M} + \text{OMe}]^-$ .

**Conversion of **3** to **1**.** A toluene solution (15 mL) of **3** (25 mg, 0.022 mmol) was refluxed for 30 min under a slow purge of  $\text{N}_2$ , during which time the color changed from red to orange. The

(35) Deeming, A. J.; Jayasuriya, S. N.; Arce, A. J.; De Sanctis, Y. *Organometallics* **1996**, *15*, 786.

(36) Arnold, L. J. *J. Chem. Educ.* **1992**, *69*, 811.

solvent was removed under reduced pressure, and the residue was taken up in  $\text{CH}_2\text{Cl}_2$  and applied to thin-layer silica plates. Elution with hexane/ $\text{CH}_2\text{Cl}_2$  (9:1 v/v) yielded compound **1** (16 mg, 90%).

**Conversion of 2 to 3 and 1.** A heptane solution (15 mL) of **2** (20 mg) was refluxed for 50 min, during which time the color changed from black to red. A similar chromatographic separation to that above developed two bands. The faster moving band gave **1**, while the slower moving band yielded the compound **3**.

**Reaction of 3 with MeCN.** A neat acetonitrile solution (20 mL) of **3** (40 mg, 0.035 mmol) was refluxed for 55 min. Upon cooling to room temperature, the solvent was rotary evaporated and the residue chromatographed on silica TLC plates. Elution with hexane/ $\text{CH}_2\text{Cl}_2$  afforded  $[(\mu_5\text{-S})\text{Ru}_5(\mu\text{-CO})_2(\text{CO})_{10}(\mu\text{-}\eta^3\text{-C}_{12}\text{H}_8\text{S})(\mu_4\text{-}\eta^2\text{-C}_6\text{H}_4)(\text{MeCN})]$  (**4**) (31 mg, 73%) as yellow crystals from hexane/ $\text{CH}_2\text{Cl}_2$  at  $-4^\circ\text{C}$ . Anal. Calcd for  $\text{C}_{32}\text{H}_{15}\text{N}_1\text{O}_{12}\text{Ru}_5\text{S}_2$ : C, 32.71; H, 1.29; N, 1.19. Found: C, 33.32; H, 1.57; N, 1.23. IR ( $\nu\text{CO}$ , KBr): 2097 w, 2066 s, 2028 vs, 1982 vs, 1965 vs, 1871 w, 1827 m  $\text{cm}^{-1}$ .  $^1\text{H}$  NMR ( $\text{CDCl}_3$ ):  $\delta$  7.78 (d,  $J = 7.6$  Hz, 1H), 7.71 (d,  $J = 7.6$  Hz, 1H), 7.52 (m, 2H), 7.36 (d,  $J = 7.4$  Hz, 1H), 7.18 (d,  $J = 7.4$  Hz, 1H), 7.05 (t,  $J = 7.2$  Hz, 1H), 6.94 (t,  $J = 7.2$  Hz, 1H), 6.78 (t,  $J = 7.2$  Hz, 1H), 6.69 (t,  $J = 7.2$  Hz, 1H), 6.23 (m, 2H), 2.39 (s, 3H). ESI-MS:  $m/z$  1194 [ $\text{M} - \text{MeCN} + \text{CO} + \text{OMe}$ ] $^-$ ; 1166 [ $\text{M} - \text{MeCN} + \text{OMe}$ ] $^-$ ; 1135 [ $\text{M} - \text{MeCN}$ ] $^-$ ; 1107 [ $\text{M} - \text{MeCN} - \text{CO}$ ] $^-$ .

**Reaction of 4 with P(OMe)<sub>3</sub>.** Compound **4** (20 mg, 0.018 mmol) was combined with  $\text{P}(\text{OMe})_3$  (one drop) in  $\text{CH}_2\text{Cl}_2$  (15 mL) and stirred for 30 min at room temperature. The solvent was rotary evaporated and the residue chromatographed as above to give  $[(\mu_5\text{-S})\text{Ru}_5(\mu\text{-CO})_2(\text{CO})_{10}(\mu\text{-}\eta^3\text{-C}_{12}\text{H}_8\text{S})(\mu_4\text{-}\eta^2\text{-C}_6\text{H}_4)\{\text{P}(\text{OMe})_3\}]$  (**5**) (0.011 g, 52%) as yellow crystals after recrystallization from hexane/ $\text{CH}_2\text{Cl}_2$  at  $-4^\circ\text{C}$ . IR ( $\nu\text{CO}$ , KBr): 2066 s, 2029 vs, 2004 vs, 1987 vs, 1958 w, 1867 m, 1830 m  $\text{cm}^{-1}$ .  $^1\text{H}$  NMR ( $\text{CDCl}_3$ ):  $\delta$  7.84 (m, 2H), 7.50 (m, 3H), 7.40 (m, 1H), 7.03 (m, 2H), 6.74 (m, 2H), 6.23 (m, 2H), 3.77 (d,  $J = 10.3$ , 9H).  $^{31}\text{P}\{^1\text{H}\}$  NMR ( $\text{CDCl}_3$ ):  $\delta$  127.7 (s). ESI-MS: (+ve ion mode)  $m/z$  1283 [ $\text{M} + \text{Na}$ ] $^+$ ; (-ve ion mode)  $m/z$  1290 [ $\text{M} + \text{OMe}$ ] $^-$ .

**X-ray Crystallography.** X-ray intensity data were collected on a Bruker SMART or a Bruker-Nonius Apex II CCD diffractometer with  $\text{Mo K}\alpha$  X-rays using standard procedures and software.

Semiempirical absorption corrections were applied (SADABS).<sup>37</sup> Structures were solved by direct methods and developed and refined on  $F^2$  using the SHELX programs<sup>38</sup> operating under WinGX.<sup>39</sup> Hydrogen atoms were included in calculated positions.

The refinement of compounds **2** and **3** were routine. For compound **1**, a final difference map revealed a significant peak ( $3.4 \text{ e } \text{\AA}^{-3}$ ) superimposed on the benzyne ligand. This could not be assigned to anything chemically sensible, so presumably arises from a small amount of disorder (perhaps by cocrystallization of a small amount of  $[(\mu_4\text{-S})_2\text{Ru}_4(\text{CO})_{11}]$ , which would be a possible byproduct in this system?). This did not affect the overall development of the structure, but will lower the precision of the bond parameters for the benzyne ligand. For cluster **4**, a half-molecule of  $\text{CH}_2\text{Cl}_2$  was located in the asymmetric unit, disordered about an inversion center, but this could be modeled successfully.

Crystallographic data for the structural analyses have been deposited with the Cambridge Crystallographic Data Centre, CCDC nos. 645272–645275. Copies of this information may be obtained free of charge from the Director, CCDC, 12 Union Rd., Cambridge CB2 1EZ, UK (fax: +44-1223-336033; e-mail: deposit@ccdc.cam.ac.uk; or <http://www.ccdc.cam.ac.uk>).

**Acknowledgment.** We thank Dr. Tania Groutso, University of Auckland, and Dr. Jan Wikaira, University of Canterbury, New Zealand, for collection of X-ray intensity data, and Dr. Viktor Moberg for the collection of the variable temperature NMR spectra of compound **1**. The Swedish International Development Agency (SIDA) and the Swedish Research Council (VR) are gratefully acknowledged for supporting the collaboration between S.E.K. and E.N.

**Supporting Information Available:** Crystallographic data. This material is available free of charge via the Internet at <http://pubs.acs.org>.

OM7004707

(37) Blessing, R. H. *Acta Crystallogr.* **1995**, *A51*, 33.

(38) Sheldrick, G. M. *SHELX97*, Programs for the solution and refinement of crystal structures; University of Göttingen: Germany, 1997.

(39) Farrugia, L. J. *WinGX*, Version 1.70.01; University of Glasgow: UK; Farrugia, L. J. *J. Appl. Crystallogr.* **1999**, *32*, 837.